Journal of Magnetic Resonance **138,** 66–73 (1999)
Article ID jmre.1999.1712, available online at http://www.idealibrary.com on IDEAL®

2D Exchange NMR Spectra under Slow MAS: A Simplified Scheme to Obtain Pure-Phase Spectra without Unwanted Cross Peaks

Matthias Ernst,*,†,[1] Arno P. M. Kentgens,* and Beat H. Meier*,†,[1]

**NSR–Center for Molecular Structure, Design, and Synthesis, Laboratory of Physical Chemistry, University of Nijmegen, Toernooiveld 1, NL-6525 ED Nijmegen, The Netherlands; and †Laboratorium für Physikalische Chemie, ETH-Zentrum, CH-8092 Zürich, Switzerland*

Received August 19, 1998; revised December 21, 1998

A simplified method for acquiring pure-phase two-dimensional exchange spectra under slow magic-angle spinning (MAS) is introduced. It combines rotor-synchronized 2D exchange spectroscopy with whole-echo acquisition leading to a simplification in data acquisition and data processing compared to the States-type data sampling using "time reversal" (A. Hagemeyer *et al., Adv. Magn. Reson.* **13, 85 (1989)). As an added benefit, it allows for well-defined mixing times of an arbitrary integer multiple of the MAS rotor period. The proposed method is, however, only applicable to samples where an echo of the free-induction decay can be obtained, i.e., where the inhomogenous linewidth is larger than the homogeneous linewidth. This is, for example, the case in rare-spin spectroscopy of samples with natural isotopic abundance. The usefulness of the new method is demonstrated, using ^{13}C spectroscopy, on two model compounds.**

Key Words: **NMR; MAS; 2D exchange; pure-phase spectra; chemical exchange; polarization exchange.**

INTRODUCTION

Two-dimensional exchange spectroscopy (*1*) plays an important role in nuclear magnetic resonance spectroscopy (NMR). 2D exchange spectroscopy can be used to investigate the topology and kinetics of chemical exchange processes, to determine internuclear distances in solids and liquids by analyzing polarization-transfer processes, and to evaluate the relative orientation of molecular segments by chemical-shielding tensor correlation in the solid state. In isotropic phase, the 2D exchange spectrum is usually recorded as an amplitude-modulated spectrum during t_1 in order to obtain pure-phase lineshapes using TPPI-type (*2, 3*) or States-type (*4*) data sampling. This requires that $+1$ and -1 quantum coherences are simultaneously selected by the phase cycle during t_1 (*5*).

The combination of two-dimensional correlation spectroscopy with magic-angle spinning (MAS) is only straightforward if the spinning speed is fast compared to the width of the chemical-shielding (CSA) tensors so that all spinning sidebands have negligible intensity. Otherwise, the naive combination of MAS and 2D exchange spectroscopy leads to cross peaks within the spinning sideband manifold of one spin (originating from one CSA tensor) even in the absence of an exchange mechanism as well as to phase distortions of the lines. In such a situation, the determination of relative tensor orientations and the detection of chemical or polarization-exchange processes between nuclei with an identical isotropic chemical shift becomes impossible. These undesired cross peaks can be avoided by performing the experiment with a rotor-synchronized mixing time and selecting -1 quantum coherence during the evolution time t_1 (*6–8*). However, this coherence-selection scheme prevents the acquisition of pure-phase two-dimensional spectra (*5*). One can resort to absolute-value mode representation of these spectra at the expense of spectral resolution.

A solution to the problem of pure phase was found by Hagemeyer *et al.* by recording four States-type amplitude-modulated data sets (*9, 10*) and combining them in a suitable way (vide infra). Two of the four data sets are recorded with the mixing time τ_m synchronized with the rotor period while the other two are recorded such that the mixing time τ_m *plus* the evolution time t_1 is synchronized with the sample rotation ("time-reversal" scheme) (*5*). Recently a modified version of the experiment was introduced where the "normal" (τ_m synchronized) and the time-reversed ($\tau_m + t_1$ synchronized) data sets are already combined during the acquisition of the data (*11*).

Whole-echo acquisition (*12*) is an alternate method to obtain pure-phase two-dimensional spectra. It is less frequently used than TPPI or States-type data acquisition since it relies on the fact that an echo of the FID can be induced (e.g., by a π pulse) without significant signal loss. Fourier transformation of such an echo signal leads to a pure absorptive spectrum with a vanishing dispersive part (*13*). The whole-echo-type acquisition of 2D data sets thus allows pure-phase two-dimensional spectra selecting either $+1$ or

[1] To whom correspondence should be addressed. Laboratorium für Physikalische Chemie, ETH-Zentrum, 8092 Zürich, Switzerland.

1090-7807/99 $30.00

-1 quantum coherence in t_1 (phase modulation). So far, whole-echo acquisition was mainly used in the context of dynamic-angle spinning (*14*) and multiple-quantum MAS (*15, 16*) of quadrupolar nuclei.

In this contribution, we describe the combination of whole-echo acquisition and rotor-synchronized 2D exchange spectroscopy to simplify the data-acquisition and processing scheme for pure-phase two-dimensional exchange spectra under slow MAS. Using whole-echo acquisition allows us to select either $+1$ *or* -1 quantum coherence during t_1 and at the same time obtain pure-phase 2D spectra. For whole-echo acquisition it is sufficient to synchronize the mixing time τ_m (or $\tau_m + t_1$) with the MAS sample rotation. It is not necessary to combine data sets obtained with slightly different rotor-synchronized mixing times and it becomes possible to acquire spectra with well-defined mixing times. The time-reversal scheme introduces irregularities in τ_m which are in the order of one rotor period. Therefore, the proposed scheme is of particular interest for experiments with short mixing times of one or a few rotor periods only.

THEORETICAL BACKGROUND

The theory of 2D correlation spectroscopy under slow magic-angle spinning has been extensively covered in the literature (*6–10*) and we only review the main points which are of relevance in connection with the whole-echo experiment. Despite the fact that the basic experiment for 2D exchange spectroscopy is an amplitude-modulated experiment, it is easier to describe the slow-spinning exchange experiment in terms of the phase-modulated signal generated by the $+1$ and -1 quantum coherences during t_1. The cosine-modulated signal of an amplitude-modulated experiment is the sum of the $+1$ and the -1 quantum coherences. In the t_2 domain, we detect -1 quantum coherence. The pathway which selects -1 quantum coherences during t_1 is sometimes referred to as "anti-echo" pathway selection while the pathway which selects $+1$ quantum coherence is referred to as "echo" pathway selection. In order to avoid confusion with the signal echo induced in our experiment (by the π pulse) we will, however, avoid these terms.

As mentioned before, the experiment described here is only of practical relevance in the absence of strong couplings and can, therefore, be analyzed in the context of a classical magnetization function. In this article we will assume that the resonance frequencies are only determined by the (anisotropic) chemical shift. For a one-dimensional experiment, the spectrum is obtained by the Fourier transform of the signal function $g^{(\pm 1)}(t) = \sum_k g_k^{(\pm 1)}(t)$, where $g_k^{(\pm 1)} = M_{k,x} \pm i \cdot M_{k,y}$ is the complex magnetization originating from spin k. The plus-and-minus signs apply for the selection of $+1$ and -1 quantum coherence, respectively.

For a two-dimensional exchange experiment, the signal function $G^{(\pm 1)}(t_1, t_2, \tau_m) = \sum_{k,l} G_{k,l}^{(\pm 1)}(t_1, t_2, \tau_m)$ is given by (*1*)

$$G_{k,l}^{(\pm 1)}(t_1, t_2, \tau_m) = C_k \cdot g_k^{(\pm 1)}(0, t_1) \cdot P_{k,l}(\tau_m) \times g_l^{(-1)}(t_1 + \tau_m, t_1 + \tau_m + t_2). \quad [1]$$

Here, $G_{k,l}^{(\pm 1)}$ is the signal contribution that oscillates, during the evolution period (t_1), with the resonance frequency of spin k and, after the mixing period of length τ_m, oscillates in the detection period t_2 with the resonance frequency of spin l. The initial polarization of spin k after excitation is denoted by C_k; $P_{k,l}(\tau_m)$ is the transfer function describing the exchange process (chemical exchange or polarization transfer) between spins k and l; and $g_k(t_a, t_b)$ is the one-dimensional signal function mentioned above but now evaluated between the time points t_a and t_b (*17*):

$$g_k^{(-1)}(t_a, t_b) = e^{-i\Omega_k(t_b - t_a)} \cdot f_k^*(\omega_r t_a) \cdot f_k(\omega_r t_b) \quad [2]$$

$$g_k^{(+1)}(t_a, t_b) = [g_k^{(-1)}(t_a, t_b)]^* = e^{+i\Omega_k(t_b - t_a)} \cdot f_k(\omega_r t_a) \cdot f_k^*(\omega_r t_b). \quad [3]$$

The first term on the right hand side of Eqs. [2] and [3] depends only on the isotropic chemical shift Ω_k while the functions $f_k(\phi)$ contain the time-dependent anisotropic chemical-shift contributions. The functions $f_k(\phi)$ depend explicitly on the anisotropy and asymmetry of the CSA tensor, the three Euler angles α, β, and γ, that describe the orientation of the crystallite in the rotor-fixed coordinate system, and the rotor angle as a function of time $\phi = \omega_r t$. The asterisk (*) denotes the complex conjugate. The functions $f_k(\phi)$ are periodic and fulfill the relationship (*17*)

$$f_k(\phi) \cdot f_k^*(\phi) = 1. \quad [4]$$

They can be expressed as a Fourier series with unit basic frequency

$$f_k(\phi) = \sum_{m=-\infty}^{\infty} d_m^k \cdot e^{+im\phi} \cdot e^{+im\gamma}. \quad [5]$$

The coefficients d_m^k depend on the principal values of the chemical-shielding tensor, the spinning speed, and the two Euler angles α and β. The dependence of $f_k(\phi)$ on the Euler angle γ is written explicitly in order to allow averaging over this angle in a later step.

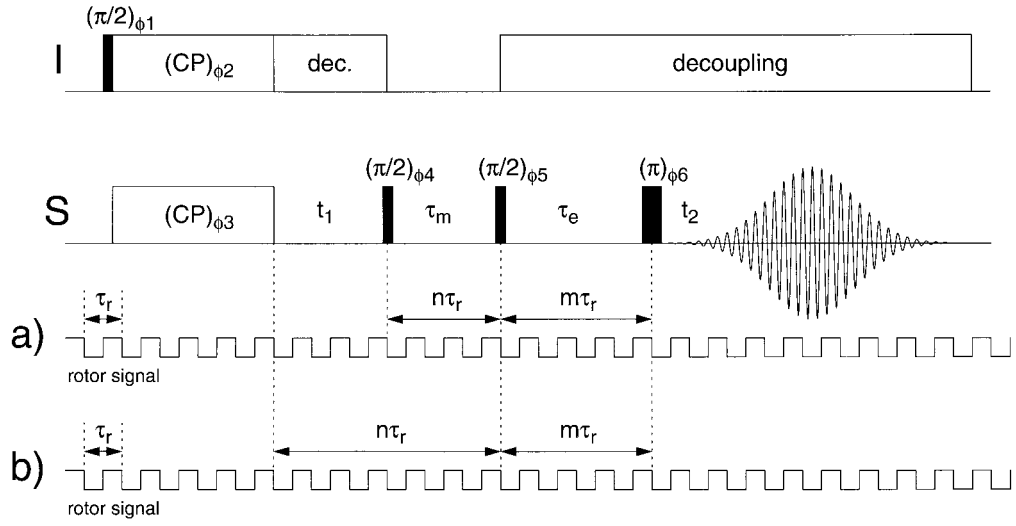

FIG. 1. Pulse sequence for the measurement of rotor-synchronized 2D exchange spectra under MAS using whole-echo acquisition. After cross-polarization, the magnetization can evolve during t_1 and is stored along the z axis for the mixing time by a $\pi/2$ pulse. The second $\pi/2$ pulse returns the magnetization into the x-y plane and the echo is generated by a π pulse. Acquisition is started directly after the final π pulse in order to record the whole echo. The synchronization of the experiment with the sample rotation is indicated below the pulse sequence. (a) shows the synchronization which is necessary for the -1 quantum coherence (t_1) -1 quantum coherence (t_2) pathway ("anti-echo" pathway). In this case the mixing time τ_m has to be an integer multiple of the rotor cycle. (b) shows the synchronization which is necessary for the $+1$ quantum coherence (t_1) -1 quantum coherence (t_2) pathway ("echo" pathway). In this case the evolution time t_1 plus the mixing time τ_m have to be an integer multiple of the rotor cycle. In both cases the echo time τ_e has to be synchronized with the sample rotation also. The phase cycle for the experiment in (a) is given by $\phi_1 = 02$, $\phi_2 = 1$, $\phi_3 = 0011$, $\phi_4 = 1$, $\phi_5 = 0000\ 1111\ 2222\ 3333$, $\phi_6 = 0$, and $\phi_R = 0213\ 3102\ 2031\ 1320$. Here, the phases are given as multiples of 90°. For the experiment in (b) only the phase ϕ_3 has to be changed to 0033.

Inserting Eq. [2] into Eq. [1] leads for the selection of -1 quantum coherence during t_1 to

$$G_{k,l}^{(-1)}(t_1, t_2, \tau_m) = C_k \cdot P_{k,l}(\tau_m) \cdot e^{-i\Omega_k t_1} \cdot e^{-i\Omega_l t_2} f_k^*(0) \times f_k(\omega_r t_1)\, f_l^*(\omega_r(t_1 + \tau_m)) \times f_l(\omega_r(t_1 + \tau_m + t_2)). \quad [6]$$

Assuming a rotor-synchronized mixing time, $\tau_m = N \cdot 2\pi/\omega_r$, we can use the periodicity of $f_k(\phi) = f_k(\phi + N \cdot 2\pi)$ to obtain

$$G_{k,l}^{(-1)}(t_1, t_2, \tau_m) = C_k \cdot P_{k,l}(\tau_m) \cdot e^{-i\Omega_k t_1} \cdot e^{-i\Omega_l t_2} f_k^*(0) \times f_k(\omega_r t_1) \cdot f_l^*(\omega_r t_1) \cdot f_l(\omega_r(t_1 + t_2)). \quad [7]$$

For the case of no transfer during the mixing period, i.e., $P_{k,l}(\tau_m) = \delta_{k,l}$, we obtain, using Eqs. [4] and [5],

$$G_{k,k}^{(-1)}(t_1, t_2, \tau_m) = C_k \cdot e^{-i\Omega_k(t_1+t_2)} \sum_{n=-\infty}^{\infty} \sum_{m=-\infty}^{\infty} d_m^k [d_n^k]^* e^{+im\omega_r(t_1+t_2)} e^{+i(m-n)\gamma}, \quad [8]$$

which clearly shows that only peaks with the same sideband order m in both dimensions t_1 and t_2 are retained. Equation [8] leads to a diagonal spectrum even for the case of a single crystallite assuming that the start of each scan is synchronized with the rotor position to ensure a constant value of γ for all evolution times t_1. The sidebands of different order m have, however, different phases since the coefficients $\sum_n d_m^k [d_n^k]^*$ are, in general, different complex numbers.

Integration over the Euler angle γ using

$$\frac{1}{2\pi} \cdot \int_0^{2\pi} d\gamma \cdot e^{-i(n-m)\gamma} = \delta_{n,m} \quad [9]$$

leads to

$$G_{k,k}^{(-1)}(t_1, t_2, \tau_m) = C_k \cdot e^{-i\Omega_k(t_1+t_2)} \sum_{n=-\infty}^{\infty} d_n^k [d_n^k]^* e^{+in\omega_r(t_1+t_2)}. \quad [10]$$

The Fourier coefficients are now all real and all sidebands have the same phase which is a prerequisite to obtain pure-phase spectra. The average over the Euler angle γ also precludes the need to synchronize the start of the scans with the rotor

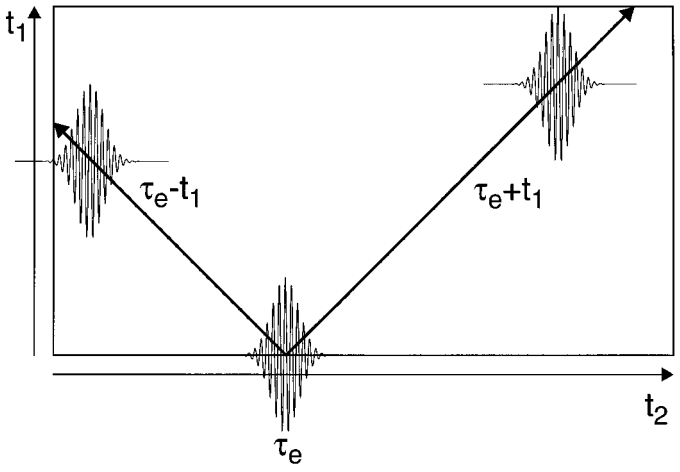

FIG. 2. Shift of the echo maximum in a 2D exchange spectrum using whole-echo acquisition and selection of -1 quantum or $+1$ quantum coherence during t_1. Selecting -1 quantum coherence during t_1 makes the echo maximum shift along the line $t_2^{\text{echo}} = \tau_e - t_1$ to shorter t_2 times for increasing values of t_1. For $+1$ quantum coherence selection during t_1 the echo maximum shifts along the line $t_2^{\text{echo}} = \tau_e + t_1$ to bigger values of t_2 for increasing t_1 times. This has the advantage that the echo time τ_e can be kept as short as possible. The origin of the t_2 time is immediately after the π pulse of the pulse sequence (see Fig. 1).

position. Averaging over the Euler angle γ is automatically obtained in a powder sample. For mixing due to chemical or magnetization exchange ($P_{k,l}(\tau_m) \neq \delta_{k,l}$), cross peaks appear. Their phase is the same as for the diagonal peaks.

If we now consider a second experiment where we select $+1$ quantum coherence during t_1 and calculate the time-domain signal we obtain the $+1$ quantum equivalent to Eq. [6] as

$$\begin{aligned} G_{k,l}^{(+1)}(t_1, t_2, \tau_m) = C_k \cdot P_{k,l}(\tau_m) \cdot e^{+i\Omega_k t_1} \cdot e^{-i\Omega_l t_2} \cdot f_k(0) \\ \times f_k^*(\omega_r t_1)\, f_l^*(\omega_r(t_1 + \tau_m)) \\ \times f_l(\omega_r(t_1 + \tau_m + t_2)). \end{aligned} \quad [11]$$

Assuming again a rotor-synchronized mixing time, expanding the functions $f_k(\phi)$ in Fourier series, simplifying to the case of no transfer during the mixing time, and averaging over the Euler angle γ lead to the signal function

$$\begin{aligned} G_{k,k}^{(+1)}(t_1, t_2, \tau_m) &= C_k \cdot e^{-i\Omega_k(t_2 - t_1)} \sum_{n=-\infty}^{\infty} \sum_{m=-\infty}^{\infty} \sum_{p=-\infty}^{\infty} \sum_{q=-\infty}^{\infty} d_n^k \\ &\quad \times [d_m^k]^* [d_p^k]^* \cdot d_q^k e^{-i(m+p-q)\omega_r t_1} \\ &\quad \times e^{+iq\omega_r t_2} \cdot e^{-i(m+p-n-q)\gamma} \\ &= C_k \cdot e^{-i\Omega_k(t_2 - t_1)} \sum_{m,p,q} d_{(m+p-q)}^k \cdot [d_m^k]^* \\ &\quad \times [d_p^k]^* \cdot d_q^k e^{-i(m+p-q)\omega_r t_1} \cdot e^{+iq\omega_r t_2}. \end{aligned} \quad [12]$$

This signal gives rise to undesired cross peaks among lines of a sideband manifold since the magnetization evolves with different resonance frequencies during t_1 and t_2.

However, if we synchronize the mixing time τ_m *plus* the evolution time t_1 by setting $(t_1 + \tau_m) \cdot \omega_r = N \cdot 2\pi$ in Eq. [11] and again take into account the periodicity of $f_k(\phi)$, we obtain after averaging over the Euler angle γ

$$\begin{aligned} G_{k,k}^{(+1)}(t_1, t_2, \tau_m) \\ = C_k \cdot e^{-i\Omega_k(t_2 - t_1)} \cdot \sum_{n=-\infty}^{\infty} d_n^k \cdot [d_n^k]^* e^{+in\omega_r(t_2 - t_1)}, \end{aligned} \quad [13]$$

which is exactly the complex conjugate of Eq. [10] with respect to the time t_1. Combining Eqs. [10] and [13] allows us to construct a cosine-modulated signal in t_1 as required for an amplitude modulated signal:

$$\begin{aligned} G_{k,k}^{\cos}(t_1, t_2, \tau_m) &= G_{k,k}^{(-1)}(t_1, t_2, \tau_m) + G_{k,k}^{(+1)}(t_1, t_2, \tau_m) \\ &= C_k \cdot e^{-\Omega_k t_2} \sum_{n=-\infty}^{\infty} d_n^k [d_n^k]^* \\ &\quad \times e^{+in\omega_r t_2} 2\cos((\Omega_k + n\omega_r)t_1). \end{aligned} \quad [14]$$

In the same way one can construct a sine-modulated signal.

The lineshape of the peak $\mathcal{S}_{k,l}(\omega_1, \omega_2) = \Im\{G_{k,l}(t_1, t_2)\}$ in the 2D spectrum can be expressed in terms of the 1D absorption mode (A_k and A_l) and dispersion mode (D_k and D_l) signals (*5*). The lineshape is given by

$$\mathcal{S}_{k,l}(\omega_1, \omega_2) = A_k(\omega_1) \cdot A_l(\omega_2) - D_k(\omega_1) \cdot D_l(\omega_2). \quad [15]$$

Two-dimensional absorption mode lineshapes are only obtained if the dispersive component vanishes, i.e., for

$$D_k(\omega_1) \cdot D_l(\omega_2) = 0. \quad [16]$$

This condition can be fulfilled in two different ways: (i) For an amplitude-modulated 2D spectrum (see Eq. [14]) this is achieved by setting $D_l(\omega_2)$ equal to zero after the first Fourier transformation using TPPI or States data processing. (ii) In the whole-echo scheme $D_l(\omega_2)$ is already zero because the Fourier transformation of a FID which is symmetric about the time origin leads to a purely absorptive signal. We can, therefore, directly use either one of the phase-modulated signals of Eqs. [10] or [13] to obtain pure-phase 2D spectra. One can either select -1 quantum coherence (anti-echo pathway selection) during t_1 and synchronize the mixing time τ_m with the rotor period or one can select $+1$ quantum coherence (echo pathway selection) during t_1 and synchronize the mixing time τ_m *plus* the evolution time t_1 with the

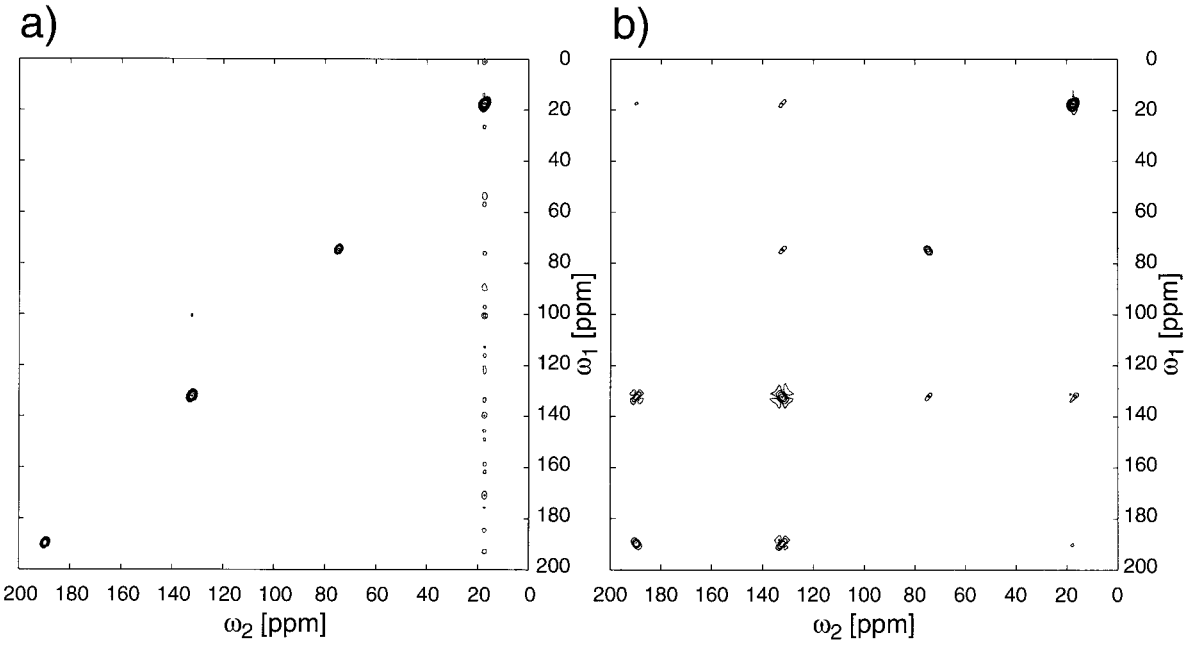

FIG. 3. Two-dimensional exchange spectra of hexamethylbenzene for a short mixing time of $\tau_m = \tau_r \approx 173$ μs. The mixing time was actively synchronized by a homebuilt electronic device. Both spectra were recorded at a MAS spinning speed of $\omega_r/(2\pi) = 5783$ Hz which corresponds to the $n = 2$ rotational-resonance condition. Five hundred twelve increments in t_1 with 16 scans each were acquired. (a) shows a spectrum with whole-echo acquisition with an echo time of $\tau_e = 20.401$ ms $(118 \cdot \tau_r)$ while (b) shows a spectrum recorded with States-type sampling without "time reversal." The States-type spectrum in (b) clearly shows the unwanted cross peaks between the center band of the aromatic carbon at 132 ppm and its first sidebands at 74.5 and 189.5 ppm, respectively, and to the resonance of the CH_3 group at 17 ppm. All lines show phase-twisted lineshapes. The whole-echo spectrum in (a) shows, as expected, only the diagonal peaks and no cross peaks since the mixing time is too short for spin diffusion to proceed. The contour levels are at 1.25, 2.5, 5, 10, 20, 40, and 80% of the maximum peak intensity. Due to the rotational-resonance condition, the sideband manifolds of the methyl and the aromatic carbons overlap.

rotor period. Advantages and disadvantages of the two schemes will be discussed in the next section.

The experiment can now be applied to exchange processes between nuclei with different tensor orientations and identical or different isotropic shifts. In these experiments, the cross peaks will bear the information about rates and pathways of the exchange process, very much like in a static sample but with higher resolution and sensitivity.

EXPERIMENTAL REALIZATION

The pulse sequence for the experimental implementation of the 2D exchange experiment under slow MAS using whole-echo acquisition is shown in Fig. 1. After cross-polarization and t_1 evolution, the magnetization is stored along the z direction by a $\pi/2$ pulse. After the mixing time τ_m the magnetization is brought back into the x-y plane by another $\pi/2$ pulse and the echo is generated by a π pulse after a time period τ_e. The acquisition is started directly after the π pulse in order to acquire the full echo. The two possible ways of synchronizing the pulse sequence with the rotor period are indicated below the pulse sequence. Figure 1a shows the rotor synchronization suitable for -1 quantum selection during t_1 (sometimes referred to as anti-echo signal selection (*5*)) while Fig. 1b shows the rotor synchronization suitable for $+1$ quantum selection during t_1 (sometimes referred to as echo signal (*5*)). Both experimental schemes give similar results. The $+1$ quantum selection during t_1 (Fig. 1b) has the advantage that the echo maximum in t_2 shifts to longer times with increasing time t_1 (Fig. 2). This allows one to choose the minimum time τ_e to acquire the whole echo. In the case of the -1 quantum selection (Fig. 1a), the echo maximum in t_2 shifts to shorter times with increasing time t_1 requiring a delay τ_e which is at least as long as t_1^{max} in order to acquire the whole echo for all desired t_1 times (Fig. 2). The drawback of the $+1$ quantum selection during t_1 is that it leads to a small variation in the length of the mixing time during the course of the experiment since the sum of $\tau_m + t_1$ is synchronized with the rotor period. The maximum deviation from the mixing time is in the order of $\tau_r/2$. For mixing times covering a large number of rotor periods, this deviation is of no practical concern; however, for short mixing times, it can become a problem.

In order to achieve a good suppression of the unwanted cross peaks, it is important to synchronize the second carbon $\pi/2$

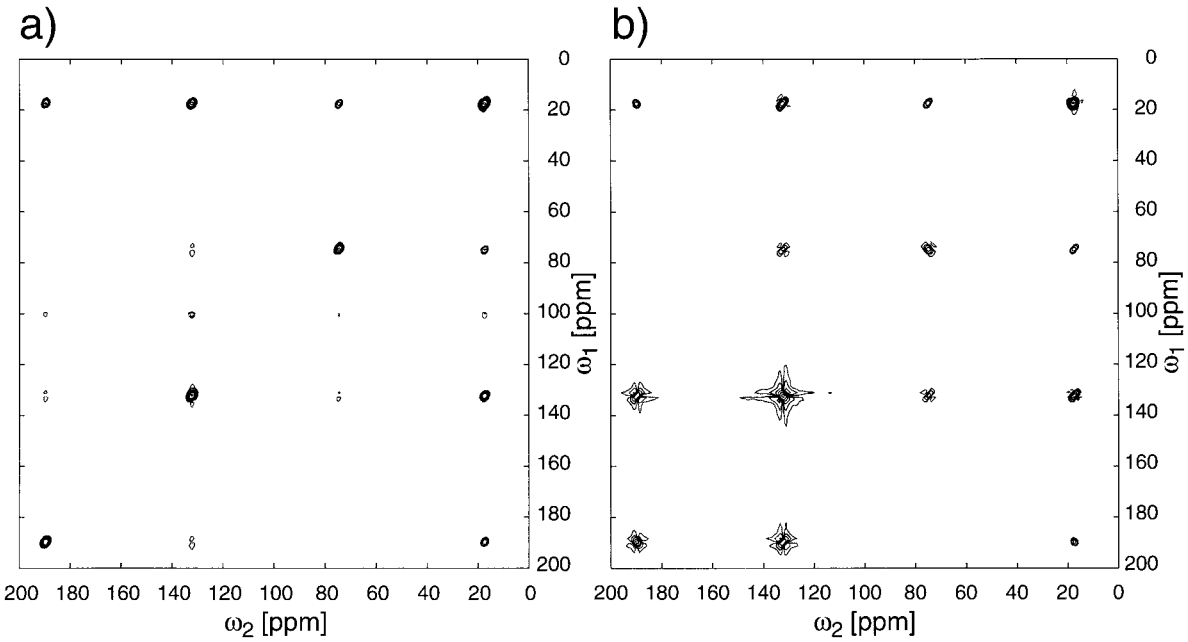

FIG. 4. Two-dimensional exchange spectra of hexamethylbenzene for a mixing time of $\tau_m \approx 2$ s. All experimental conditions except for the number of scans (32 per t_1 increment) were the same as in Fig. 3. The whole-echo spectrum (a) shows strong cross peaks between the three lines of the aromatic carbons and the CH_3 group. However, there are only very weak cross peaks between the center band and the sidebands of the aromatic carbon at a level of about 1% of the maximum peak intensity. They are due to imperfect rotor synchronization. The States-type spectrum without "time reversal" (b) shows strong sidebands between all the resonances except for the $+1$ and -1 sideband of the aromatic carbons. The peaks have strongly phase-twisted lineshapes. The contour levels are at 1.25, 2.5, 5, 10, 20, 40, and 80% of the maximum peak intensity. Due to the rotational-resonance condition, the sideband manifolds of the methyl and the aromatic carbons overlap.

pulse *and* the π pulse, which generates the echo signal with a high precision. Deviations from the exact multiple of a rotor cycle as small as 2° produce strong additional cross-peak signals as well as small phase twists in the lineshapes. This implies that for mixing times long compared to a rotor cycle, active synchronization of the basic 2D exchange sequence with the rotor cycle is required, i.e., measuring the position of the rotor and restarting the pulse programmer at the stored rotor position. For the additional echo time, τ_e, which is chosen as short as possible and thus never exceeds a few rotor periods, passive synchronization is sufficient if the spinning speed is reasonably stable, i.e., it is sufficient to set the mixing time to a multiple of the rotor cycle.

There are two important consequences for the processing of data sets acquired with whole-echo acquisition. First, the maximum of the window function is a function of t_1 and needs to be shifted the same way as the echo maximum is shifting (see Fig. 2). Second, a first-order phase correction is necessary because the origin of the time axis is not at the start of the acquisition but at the echo maximum.

RESULTS AND DISCUSSION

In order to demonstrate the usefulness of the method, we have recorded polarization-exchange (rotor-driven spin-diffusion) spectra and spectra showing exchange due to molecular reorientation.

Rotor-driven 2D spin-diffusion spectra of hexamethylbenzene at the $n = 2$ rotational-resonance condition (*18*, *19*) are presented in Figs. 3 and 4. Under this condition the ^{13}C spin-diffusion process in hexamethylbenzene at natural isotopic abundance is fast enough to produce significant cross-peak intensity for mixing times in the order of a few seconds. For a short mixing time (one rotor period) no spin diffusion takes place and the whole-echo acquisition leads, as expected, to a cross-peak-free two-dimensional spectrum (Fig. 3a) while the spectrum acquired with States-type sampling without time reversal (Fig. 3b) shows the unwanted cross peaks due to the selection of $+1$ quantum and -1 quantum coherence during t_1. The crystal structure of hexamethylbenzene belongs to the $P\bar{1}$ space group (*20*) with a single molecule per unit cell. The experiments were carried out at room temperature where the reorientation of the hexamethylbenzene around the sixfold axis is fast on the NMR timescale. We expect, therefore, no cross peaks between the different sidebands (neither by chemical exchange nor by spin diffusion to neighboring molecules) of the aromatic carbon even for longer mixing times.

Figure 4 shows the same two spectra acquired with a longer mixing time of 2 s. During this time spin diffusion will lead to

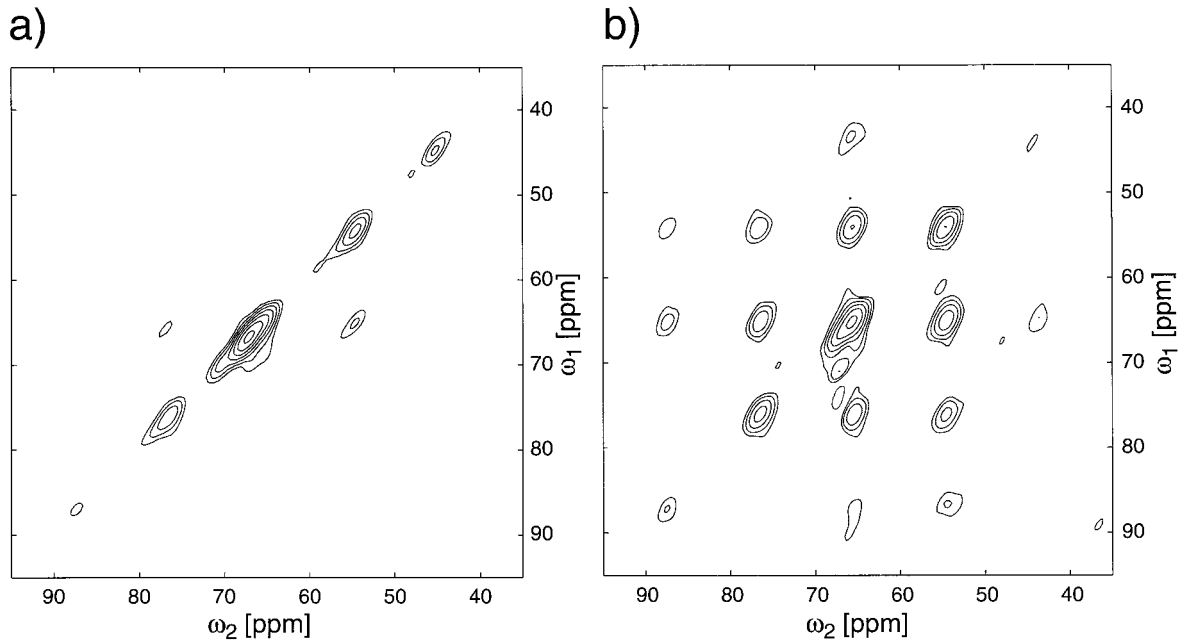

FIG. 5. Two-dimensional exchange spectra of polyoxymethylene (Delrin) at a spinning speed of $\omega_r/(2\pi) = 1100$ Hz at a temperature of $T \approx 80°C$. One hundred twenty-eight t_1 increments with 32 (a) and 128 (b) scans were acquired using an echo time of $\tau_e = 10 \cdot \tau_r \approx 9.084$ ms. The mixing times were (a) $\tau_m \approx 909$ μs and (b) $\tau_m \approx 2$ s. The mixing time was actively synchronized using a homebuilt electronic device. The spectrum in (a) with a short mixing time shows almost no cross peaks between the spinning sidebands (center-band frequency 67 ppm) while the spectrum in (b) with a long mixing time shows strong cross peaks among the spinning sidebands of the CH_2 group due to the screw-type rotation motion of the polyoxymethylene chains. The lineshape of all the peaks is purely absorptive. The contour levels are at 1.25, 2.5, 5, 10, 20, 40, and 80% of the maximum peak intensity.

a transport of polarization between the methyl and the aromatic ^{13}C spins. The whole-echo spectrum (Fig. 4a) indeed shows clear cross peaks between the CH_3 resonance and the aromatic spinning sideband manifold. Cross peaks within the aromatic spinning sideband manifold are negligible. Clearly all lines in the whole-echo spectrum have pure phase. The States-type spectrum, again without time reversal (Fig. 4b) shows the expected strongly phase-twisted lineshapes for the diagonal and the cross peaks. Moreover, it shows additional strong cross peaks among the spinning sidebands of the aromatic resonance. The spectra in Figs. 3a and 4a were recorded by selecting the -1 quantum coherence during t_1, i.e., with the experimental scheme shown in Fig. 1a where the mixing time τ_m is synchronized with the sample rotation.

As a second example we have measured the 2D exchange spectrum of polyoxymethylene at a temperature of $T \approx 80°C$. At this temperature the crystalline part of the polymer shows a screw-type motion which leads to cross peaks between the sidebands due to different orientations of the chemical-shielding tensors (*8*). At a mixing time of $\tau_m \approx 909$ μs (Fig. 5a) there are almost no cross peaks visible and the diagonal is purely absorptive. For a longer mixing time of $\tau_m \approx 2$ s strong cross peaks between the spinning sidebands of the chemical-shielding tensor can be seen. All peaks still show pure absorptive lineshapes. These spectra were recorded by selecting $+1$ quantum coherence during t_1, i.e., with the experimental scheme shown in Fig. 1b where the mixing time τ_m *plus* the evolution time t_1 was actively synchronized with the sample rotation by measuring the position of the rotor.

The application of the whole-echo method relies on the possibility of generating an echo by applying a π pulse to the system. This limits the application of the proposed method to systems where the decay of the FID is not determined by the T_2 relaxation time of the observed spins but by an inhomogenous broadening which can be refocused by a π pulse. In systems with high-abundant nuclei or in uniformly labeled materials the homonuclear *J*-coupling and the homonuclear dipolar coupling limit the application of the whole-echo method since these interactions cannot be refocused by a π pulse. However, for observing chemical-exchange processes the proposed method opens a simpler alternative to acquire pure-phase two-dimensional exchange spectra under slow MAS. In systems where the minimum number of scans per t_1 increment is dictated by the length of the phase cycle and not by the required signal-to-noise ratio, the whole-echo acquisition has the added benefit that only one data set is required. This leads to a reduction of the required measurement time.

CONCLUSIONS

We have shown that it is possible to combine whole-echo acquisition with two-dimensional exchange spectroscopy un-

der slow MAS to obtain pure-phase spectra. Compared to the method using States-type data acquisition and time reversal, only one instead of two or four different data sets must be acquired. This makes data acquisition and data processing considerably simpler. If the minimum number of scans is limited by the phase cycle, this also leads to a possible savings in time. The whole-echo method allows, in addition, the use of well-defined mixing times of an integer multiple of the rotor period if the -1 quantum coherence pathway is selected during t_1. This can be an advantage for short mixing times of a few rotor cycles.

ACKNOWLEDGMENTS

Financial support from SON and the SON National HF-NMR Facility, University of Nijmegen, and technical support by J. van Os, H. Janssen, and G. Nachtegaal are gratefully acknowledged. We also thank Dr. Susan M. De Paul for carefully reading the manuscript.

REFERENCES

1. J. Jeener, B. H. Meier, P. Bachmann, and R. R. Ernst, *J. Chem. Phys.* **71,** 4546 (1979).
2. G. Drobny, A. Pines, A. Sinton, D. Weitekamp, and D. Wemmer, *Symp. Faraday Soc.* **13,** 49 (1979).
3. D. Marion and K. Wüthrich, *Biochem. Biophys. Res. Commun.* **113,** 967 (1983).
4. D. J. States, R. A. Haberkorn, and D. J. Ruben, *J. Magn. Reson.* **48,** 286 (1982).
5. R. R. Ernst, G. Bodenhausen, and A. Wokaun, "Principles of Nuclear Magnetic Resonance in One and Two Dimensions," Clarendon Press, Oxford (1987).
6. A. de Jong, A. P. M. Kentgens, and W. S. Veeman, *Chem. Phys. Lett.* **109,** 337 (1984).
7. A. P. M. Kentgens, A. de Jong, E. de Boer, and W. S. Veeman, *Macromolecules* **18,** 1045 (1985).
8. A. P. M. Kentgens, E. de Boer, and W. S. Veeman, *J. Chem. Phys.* **87,** 6859 (1987).
9. A. Hagemeyer, K. Schmidt-Rohr, and H. W. Spiess, *Adv. Magn. Reson.* **13,** 85 (1989).
10. Z. Luz, H. W. Spiess, and J. J. Titman, *Isr. J. Chem.* **32,** 145 (1992).
11. G. J. Boender and S. Vega, *J. Magn. Reson.* **133,** 281 (1998).
12. A. Bax, A. F. Mehlkopf, and J. Smidt, *J. Magn. Reson.* **35,** 373 (1979).
13. R. Bracewell, "The Fourier Transform and Its Applications," McGraw–Hill, New York (1965).
14. P. J. Grandinetti, J. H. Baltisberger, A. Llor, Y. K. Lee, U. Werner, M. A. Eastman, and A. Pines, *J. Magn. Reson. A* **103,** 72 (1993).
15. D. Massiot, B. Touzo, D. Trumeau, J. P. Coutures, J. Virlet, P. Florian, and P. J. Grandinetti, *Solid State Nucl. Magn. Reson.* **6,** 73 (1996).
16. S. P. Brown and S. Wimperis, *J. Magn. Reson.* **124,** 279 (1997).
17. K. Schmidt-Rohr and H. W. Spiess, "Multidimensional Solid-State NMR and Polymers," Academic Press, London (1994).
18. M. G. Colombo, B. H. Meier, and R. R. Ernst, *Chem. Phys. Lett.* **146,** 189 (1988).
19. D. P. Raleigh, M. H. Levitt, and R. G. Griffin, *Chem. Phys. Lett.* **146,** 71 (1988).
20. L. O. Brockway and J. M. Robertson, *J. Chem. Soc.* **1939,** 1324 (1939).